ACS Catalysis

pubs.acs.org/acscatalysis Research Article

Thermodynamics-Driven Production of Value-Added D-Allulose from Inexpensive Starch by an *In Vitro* Enzymatic Synthetic Biosystem

Yunjie Li,[&] Ting Shi,[&] Pingping Han, and Chun You*

Cite This: *ACS Catal.* 2021, 11, 5088−5099

ABSTRACT: D-Allulose, which can be used as a food additive or functional food, is an important low-calorie functional rare sugar. The current commercial production of D-allulose is performed through the epimerization of fructose by D-allulose 3-epimerase. However, due to the inherent reaction equilibrium of this conversion, this method suffers from a low conversion yield (lower than 40%), leading to a high production cost. In this study, an *in vitro* synthetic enzymatic biosystem based on phosphorylation-dephosphorylation enzymatic cascade conversion routes for the thermodynamics-driven production of D-allulose from low-cost starch was designed and constructed. By optimizing the reaction conditions, the yield of D-allulose from 10 g/L starch reached 88.2%. To investigate the potential use of this *in vitro* synthetic enzymatic biosystem for the production of D-allulose on an industrial scale, D-allulose was synthesized from 50 g/L starch (275 mM glucose equivalent) with a product yield of 79.2%. These results indicated that the product cost of D-allulose could be decreased significantly through this strategy. In addition to D-allulose, this thermodynamics-driven strategy may also provide a promising alternative for the cost-efficient production of many other rare sugars (e.g., tagatose, mannitol, and sorbitol) on an industrial scale.

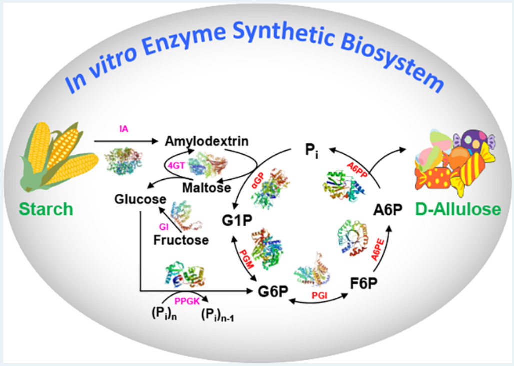

KEYWORDS: *D-allulose, starch, D-allulose 6-phosphate, in vitro enzyme synthetic biosystem, D-allulose 6-phosphate phosphatase*

■ INTRODUCTION

Currently, the incidence and prevalence of some diseases, including obesity, hyperlipidemia, hypertension, and diabetes, have dramatically increased worldwide. Sugar overconsumption and high-fat diets are considered among the most causative factors for this situation.[1] As a result, low-calorie rare sugars, which are defined as monosaccharides and their derivatives by the International Society of Rare Sugars (ISRS) that rarely exist in nature,[2−4] have attracted much attention for their application in the food, feed, pharmaceutical, medicine, synthetic chemistry, and pest control industries.[5−7] D-Allulose (also called D-psicose) is a low-calorie functional rare sugar and the C-3 epimerization product of fructose. It exists in small amounts as a free sugar in agricultural products[8,9] and as a nonfermentable component of commercial foodstuffs.[10] D-Allulose has 70% relative sweetness and only 10% of the calories of sucrose, and it is considered an ideal substitute for sucrose and high fructose corn syrup (HFCS).[11] Importantly, D-allulose has recently been generally recognized as safe (GRAS) by the Food and Drug Administration (FDA) (GRN No. 400, 498, 693, and 755). D-Allulose has also been granted permission as a food additive in a series of foods and dietary supplements, such as ice cream, chocolate, and sauce, thus showing its high promising market potential. In addition to food additives, D-allulose also has distinctive physicochemical properties and physiological functions, such as antihyperlipidemic effects,[12] antihyperglycemic effects,[13,14] anti-inflammatory effects,[15] neuroprotective effects,[16] reactive oxygen species (ROS) scavenging activity,[17] and therapeutic effects against atherosclerosis.[18] Moreover, this rare sugar can enhance gel strength, decrease the oxidation extent, and improve flavor during food processing.[19]

D-Allulose can be synthesized by chemical methods,[20,21] which suffer from sophisticated purification processes and the generation of chemical wastes and by-products. In recent years, massive efforts have been devoted to the biosynthesis of D-allulose from fructose by sugar 3-epimerase based on the Izumoring isomerization strategy.[22] Fructose can be produced from widespread and low-cost starch (starch can be converted to glucose by amylase and α-glucosidase; glucose can be converted to fructose by glucose isomerase with a product yield of ∼50%) and sugar 3-epimerases, including D-psicose 3-epimerase family enzymes, D-tagatose 3-epimerase family enzymes, and L-ribulose 3-epimerase family enzymes, which can be found in many microorganisms using bioinformatics

Received: December 31, 2020
Revised: March 25, 2021

https://doi.org/10.1021/acscatal.0c05718
ACS Catal. 2021, 11, 5088−5099

tools.[22] Thus, D-allulose is the most accessible rare sugar. The Gibbs energy change of converting fructose to D-allulose is ~0.1 kJ/mol (http://equilibrator.weizmann.ac.il/), indicating that approximately 50% of fructose can be converted to D-allulose,[23] although the actual value is lower than 40%.[5] Several approaches have been applied to improve the shift conversion of fructose to D-allulose, such as the addition of borate to break the reaction equilibrium[24] and separation by simulated moving bed chromatography (SMB).[25,26] Nevertheless, these processes suffer from complicated product separation and excessive equipment investment, resulting in the high production cost of D-allulose. Therefore, it is of great interest to develop a highly efficient and low-cost green biomanufacturing method for D-allulose production.

In vitro synthetic enzymatic biosystems consist of several cascade enzymes for implementing complicated biochemistry reactions from renewable inexpensive substrates to products, and they have emerged as important manufacturing platforms.[27] Recently, thermodynamics-driven production of many value-added chemicals with high yields by *in vitro* synthetic enzymatic biosystems has been realized.[28] In these biosystems, inexpensive oligosaccharides, such as starch and cellulose, were used as substrates for phosphorylation to generate glucose 1-phosphate (G1P) by glucan phosphorylase followed by the conversion of sugar-phosphate *via* isomerization, epimerization, and cyclization by isomerase, epimerase, and synthase, respectively. The last step of these biosystems is the dephosphorylation reaction, which is irreversible, and the theoretical yield of the final product could be close to 100%.[29] This strategy for constructing an *in vitro* synthetic enzymatic biosystem provides a promising approach to circumventing the low conversion yield of D-allulose synthesis based on the Izumoring strategy.

In this study, an *in vitro* synthetic enzymatic biosystem based on "the thermodynamics-driven strategy" was constructed for D-allulose biosynthesis from low-cost starch. This biosystem contained five core enzymes, i.e., α-glucan phosphorylase (αGP), phosphoglucomutase (PGM), phosphoglucose isomerase (PGI), D-allulose 6-phosphate 3-epimerase (A6PE), and D-allulose 6-phosphate phosphatase (A6PP), and four auxiliary enzymes, i.e., isoamylase (IA), 4-α-glucanotransferase (4GT), polyphosphate glucokinase (PPGK), and glucose isomerase (GI). After the optimization of the reaction conditions, the production yields of D-allulose from 10 and 50 g/L starch reached 88.2 and 79.2%, respectively. This method enables the preparation of difficult-to-access rare sugars from common and inexpensive starting materials in high yields without the need for labor-intensive isomer separation steps.

MATERIALS AND METHODS

Chemicals. All chemicals were of reagent grade and purchased from Sigma-Aldrich (St. Louis, MO, USA) and Sinopharm (Shanghai, China) unless otherwise noted. The dextrose equivalent of maltodextrin was 4.0−7.0. The Luria−Bertani (LB) medium was used for *Escherichia coli* cell growth and recombinant protein expression supplemented with 100 μg/mL ampicillin or 50 μg/mL kanamycin. Oligonucleotides were synthesized by GENEWIZ. Glucose isomerase (GI) was purchased from Novozymes (Denmark), and the product name was Sweetzyme IT Extra.

Expression and Purification of Enzymes. *E. coli* Top10 was used for DNA manipulation, and *E. coli* BL21 (DE3) was used for recombinant protein expression. The following three plasmids were previously described: pET20b-TmαGP encoding α-glucan phosphorylase (αGP) from *Thermotoga maritima*, pET20b-TkPGM encoding phosphoglucomutase (PGM) from *Thermococcus kodakarensis*, and pET28a-TtcPGI encoding phosphoglucose isomerase (PGI) from *Thermus thermophilus*.[30] The plasmids pET20b-A6PE with an expression cassette containing D-allulose 6-phosphate 3-epimerase (A6PE) from *Thermoanaerobacterium thermosaccharolyticum* DSM 571 and *Thermotogae* bacterium were obtained through gene synthesis after codon optimization by GENEWIZ. The plasmids pET20b-A6PP with an expression cassette containing D-allulose 6-phosphate phosphatase (A6PP) from *Acidothermus cellulolyticus*, *E. coli*, *Streptomyces avermitilis* MA-4680, *Bacteroides fragilis* NCTC 9343, *Clostridium thermocellum*, *Thermotoga maritima* MSB8, *Thermoanaerobacter wiegelii*, *Aquifex aeolicus*, and *Caldanaerobacter subterraneus* were obtained through gene synthesis after codon optimization by GENEWIZ.

E. coli BL21 (DE3) harboring the expression vector was cultured in an LB medium supplemented with the appropriate antibiotic at 37 °C until reaching an optical density at 600 nm of 0.8−1.0. Recombinant protein overexpression was induced with 0.01−0.5 mM isopropyl-β-D-thiogalactopyranoside (IPTG) for another 20 h at 18 °C. The cells were harvested by centrifugation at 4 °C and washed once with 50 mM HEPES buffer (pH 7.0) containing 0.1 M NaCl. The cell pellets were resuspended in the same buffer to a final OD_{600} of 50 and lysed by high-pressure homogenization at 4 °C. After centrifugation, the target enzymes in the supernatants were purified. Affinity adsorption on charged nickel resins was used to purify αGP, PGM, PGI, and A6PPs, and affinity adsorption on charged cobalt resins was used to purify A6PEs because the nickel ion was reported to have the possibility to inhibit the activity of A6PE.[31] For D-allulose production by *in vitro* multienzymatic reactions, heat precipitation at 70 °C for 30 min was used to purify αGP, PGM, and PGI, and heat precipitation at 60 °C for 30 min was used to purify TtA6PE and CtA6PP. Glycerol was added to the purified enzymes at a final concentration of 5% and stored at −20 °C for further use.

Enzyme Activity Assays. All the enzymes for converting starch to D-allulose are summarized in Table S1. The specific activities of αGP, PGM, and PGI were measured as previously described.[30] The specific activity of A6PE was measured at 50 °C in 100 mM HEPES buffer (pH 7.0) containing 5 mM $MgCl_2$, 10 mM fructose 6-phosphate (F6P), 2.0 U/mL CtA6PP, and an appropriate amount of A6PE. The reaction was started with the addition of A6PE and stopped in an ice-water bath. The released inorganic phosphate was measured by a mild pH phosphate assay.[32] The monosaccharide epimerization activity of converting D-allulose to fructose by A6PE was measured at 55 °C in 100 mM HEPES buffer (pH 7.0) containing 5 mM $MgCl_2$, 10−3750 mM D-allulose, and 0.5 g/L TtA6PE for 10 min. The reaction was stopped by boiling for 1 min, and the product fructose was detected by a coupling enzymatic method. The assay was performed in 100 mM HEPES buffer (pH 7.5) containing 5 mM $MgCl_2$, 0.5 mM $MnCl_2$, 2 mM NAD^+, 2 mM ATP, 5.0 U/mL hexokinase (HK), 5.0 U/mL PGI, and 5.0 U/mL glucose 6-phosphate dehydrogenase (G6PDH) at 25 °C for 10 min. The increase in the absorbency of NADH at 340 nm has a linear relationship with the concentration of fructose in the reaction solution (R^2 = 0.9998); therefore, this method can be used to determine the concentration of fructose. One unit (U) of enzyme activity was

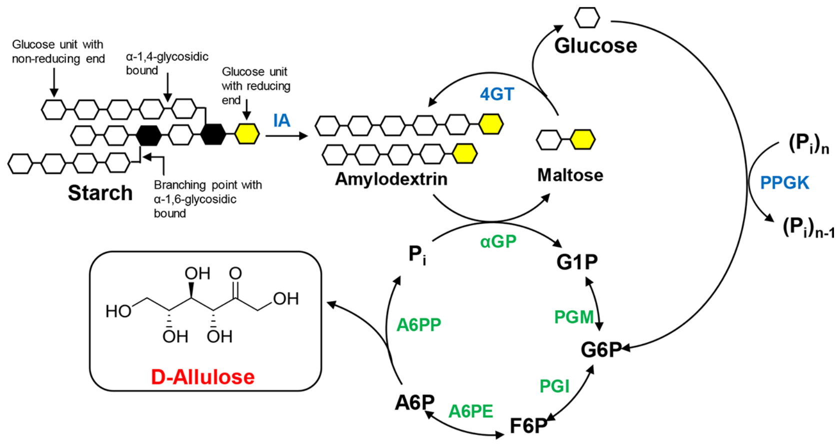

Figure 1. Schematic representation of the production of D-allulose from starch *via* an *in vitro* synthetic enzymatic biosystem. The five core enzymes include α-glucan phosphorylase (αGP), phosphoglucomutase (PGM), phosphoglucose isomerase (PGI), D-allulose 6-phosphate epimerase (A6PE), and D-allulose 6-phosphate phosphatase (A6PP), and the auxiliary enzymes include 4-α-glucanotransferase (4GT), polyphosphate glucokinase (PPGK), and isoamylase (IA). The intermediates are abbreviated as follows: A6P, D-allulose 6-phosphate; F6P, fructose 6-phosphate; G6P, glucose 6-phosphate; G1P, glucose 1-phosphate; P_i, inorganic phosphate; $(P_i)_n$ or $(P_i)_{n-1}$, polyphosphate.

defined as the amount of enzyme that generated 1 μmol of fructose per minute.

The specific activity of A6PP on D-allulose 6-phosphate (A6P) was measured in 100 mM HEPES buffer (pH 7.0) containing 5 mM $MgCl_2$, 10 mM F6P, 10.0 U/mL TtA6PE, and an appropriate amount of A6PP (test group), and the components in the control experiment were the same as the test group without adding TtA6PE. The specific activity of A6PP on D-allulose 6-phosphate is characterized by the amount of inorganic phosphate released in the reaction. The specific activities of A6PP on glucose 1-phosphate (G1P), glucose 6-phosphate (G6P), and fructose 6-phosphate (F6P) were also measured under the same conditions without TtA6PE. The reaction was started with the addition of A6PP and stopped in an ice-water bath. The released inorganic phosphate was measured by the mild pH phosphate assay.[32] One unit (U) of enzyme activity was defined as the amount of enzyme that released 1 μmol of phosphate per minute.

One-Pot Biosynthesis of D-Allulose. Ultrafiltration using the Amicon Ultra Centrifugal filter with a molecular weight cutoff of 3 kDa was carried out several times to remove the glycerol in the enzyme storage buffer. Before the proof-of-concept experiment of converting maltodextrin to D-allulose, the substrate of maltodextrin (DE = 4−7) was pretreated with IA at 80 °C for 2.5 h (S/E = 1500:1). The proof-of-concept experiment was performed in 10 mM sodium phosphate buffer (pH 7.5) containing five-enzyme cocktails with 2.0 U/mL of each enzyme, 5 mM $MgCl_2$, and 10 g/L isoamylase (IA)-treated maltodextrin (55 mM glucose equivalent). The reaction was performed at 50 °C for 24 h. An aliquot (200 μL) of the reaction sample was withdrawn and then mixed with 11 μL of 10% H_2SO_4 to stop the reaction. HPLC was then applied to determine the product concentration.

The reaction time was set as 4 h for the optimization of reaction conditions as this time node is the turning point that the reaction rate began to decrease significantly according to the results of the proof-of-concept experiment. Different buffer pH values, such as pH 6.0, 6.5, 7.0, 7.5, and 8.0, were tested for the reaction at 50 °C for 4 h to determine the optimal pH. Reaction temperatures of 50, 55, and 60 °C were applied to determine the optimal temperature.

Enzyme loading amounts were optimized using a titration method in 10 mM sodium phosphate buffer (pH 7.0), 5 mM $MgCl_2$, 55 mM glucose equivalent IA-treated maltodextrin (10 g/L) plus a five-enzyme cocktail. The concentration of D-allulose was determined at a reaction time of 4 h. The concentration of TmαGP was varied from 0.1 to 5.0 U/mL, while the other four enzymes were loaded at 2.0 U/mL for each. After the optimal loading amount of TmαGP was set, the TkPGM concentration was changed from 0.1 to 5.0 U/mL while the other three enzymes, TtcPGI, TtA6PE, and CtA6PP, were each loaded at 2.0 U/mL. After the optimal loading amounts of TmαGP and TkPGM were both set, the concentration of TtcPGI was adjusted from 0.1 to 5.0 U/mL while TtA6PE and CtA6PP were loaded at 2.0 U/mL. Then, after the optimal loading amounts of TmαGP, TkPGM, and TtcPGI were set, TtA6PE was varied from 0.1 to 5.0 U/mL while CtA6PP was loaded at 2.0 U/mL. Finally, after the concentrations of TmαGP, TkPGM, TtcPGI, and TtA6PE were set, the concentration of CtA6PP was varied from 0.1 to 5.0 U/mL to determine the optimal loading amount.

For the complete utilization of starch to produce D-allulose, 4-α-glucanotransferase (4GT), polyphosphate glucokinase (PPGK), and glucose isomerase (GI) were added. Reactions were first performed under the optimal conditions with 55 mM glucose equivalent isoamylase (IA)-treated maltodextrin (10 g/L) and five core enzymes for 6 h, and then 2.0 U/mL Tl4GT, 2.0 U/mL TfuPPGK, 2.0 U/mL GI, 12 mM polyphosphate, and 12 mM $MgCl_2$ were added to the reaction mixture. The concentrations of glucose, fructose, and D-allulose at 24 h were determined by HPLC to evaluate the effect of adding auxiliary enzymes.

Conversion of a High Concentration of Maltodextrin int D-Allulose. A high concentration of maltodextrin (50 g/L) was used for D-allulose production. The reaction was carried out in 30 mM sodium phosphate buffer (pH 7.0) at 55 °C containing 5 mM $MgCl_2$, 275 mM glucose equivalent isoamylase (IA)-treated maltodextrin (50 g/L), 10.0 U/mL TmαGP, 2.5 U/mL TkPGM, 2.5 U/mL TtcPGI, 10.0 U/mL TtA6PE, and 15.0 U/mL CtA6PP for 24 h. After the reaction proceeded for 5 h, 10.0 U/mL Tl4GT, 10.0 U/mL TfuPPGK, 10.0 U/mL GI, 60 mM polyphosphate, and 60 mM $MgCl_2$ were added to the reaction solution.

https://doi.org/10.1021/acscatal.0c05718
ACS Catal. 2021, 11, 5088−5099

Table 1. Screening of D-Allulose 6-Phosphate 3-Epimerase

enzyme name	source and its optimum growth temperature	UniProt entry number	sequence similarity with P32719	specific activity (U/mg at 50 °C)	ref
D-allulose 6-phosphate 3-epimerase (A6PE)	*Escherichia coli* K-12 MG1655 (37 °C)	P32719			31
	Thermoanaerobacterium thermosaccharolyticum DSM 571 (60 °C)	D9TQJ4	53.4%	132.6 ± 1.2	this study
	Thermotogae bacterium (80 °C)	A0A3D6DDL0	35.8%	17.4 ± 0.9	this study

Other Assays. Glucose, fructose, and D-allulose were determined by HPLC equipped with a Bio-Rad HPX-87H column and a refractive index detector. The column at 60 °C was eluted with a mobile phase of 5 mM H_2SO_4 at a flow rate of 0.6 mL/min. The purity of the recombinant proteins was checked by 12% SDS-PAGE (Figure S3). Protein concentrations were determined by the Bio-Rad Bradford protein dye reagent method (Bio-Rad, Hercules, CA, USA) with bovine serum albumin (BSA) as the standard.

RESULTS

***In Vitro* Pathway Design for D-Allulose Production.** An *in vitro* synthetic enzymatic biosystem based on the thermodynamics-driven cascade reaction was designed and constructed for the cost-efficient transformation of starch to D-allulose (Figure 1 and Table S1). This biosystem contains five core enzymes, and the following reactions occur: (1) phosphorylation of maltodextrin (a derivative of starch) to glucose 1-phosphate (G1P) catalyzed by α-glucan phosphorylase (αGP) in the presence of inorganic phosphate, (2) conversion of G1P to glucose 6-phosphate (G6P) catalyzed by phosphoglucomutase (PGM), (3) conversion of G6P to fructose 6-phosphate (F6P) catalyzed by phosphoglucose isomerase (PGI), (4) epimerization of F6P to D-allulose 6-phosphate (A6P) catalyzed by D-allulose 6-phosphate 3-epimerase (A6PE), and (5) dephosphorylation of A6P to D-allulose and inorganic phosphate catalyzed by D-allulose 6-phosphate phosphatase (A6PP). Inorganic phosphate can be recycled between reactions 1 and 5 in one vessel. Furthermore, to achieve the complete utilization of maltodextrin for D-allulose production, auxiliary enzymes, namely, isoamylase (IA), 4-α-glucanotransferase (4GT), and polyphosphate glucokinase (PPGK), are added to the reaction solution at different timepoints.[33] IA is used to debranch maltodextrin to break down α-1,6-glycosidic linkages, thus yielding linear amylodextrin. The chain length of amylodextrin continuously decreases as G1P is generated until amylodextrin becomes maltose, which is not utilized by αGP. More G1P can be generated from maltose with the help of 4GT. The enzyme 4GT can rearrange one anhydroglucose unit from maltose to another maltose to yield short-chain amylodextrin and glucose, in which short-chain amylodextrin can be utilized by αGP for the generation of G1P. All glucose molecules released from transglycosylation by 4GT could be converted to G6P catalyzed by PPGK in the presence of polyphosphate. Thus, all the glucose units of maltodextrin could be converted to D-allulose by this *in vitro* biosystem.

This *in vitro* enzymatic starch phosphorylation utilizes phosphate and α-1,4-glycosidic bond energy from starch to activate glucose units. It enables the cost-effective production of G6P by avoiding the use of costly ATP and utilizing all glucose units of starch for D-allulose production. The consolidation of starch phosphorylation, isomerization, epimerization, and irreversible dephosphorylation to D-allulose has an overall $\Delta G'^0$ of −13.2 kJ/mol (http://equilibrator.weizmann.ac.il/). In particular, the $\Delta G'^0$ of A6P dephosphorylation to D-allulose and inorganic phosphate is −15.5 kJ/mol, indicating that the last step reaction for D-allulose production is thermodynamically favorable and unidirectional to push the overall reaction toward completeness. The thermodynamic analysis of this *in vitro* biosystem indicates the nearly 100% theoretical product yield of D-allulose from starch.

Enzyme Selection and Mining of A6PP and A6PE. For *in vitro* synthetic biosystems, thermostable enzymes are desired as building blocks because the usage of thermostable enzymes can prolong the lifetime of enzymes, decrease microbial contamination odds, and simplify the operation process.[34] In this *in vitro* biosystem that converts starch to D-allulose, αGP from *Thermotoga maritima* MSB8, PGM from *Thermococcus kodakarensis*, and PGI from *Thermus thermophilus* HB8 have been well characterized and widely used in the *in vitro* production of inositol, fructose 1,6-diphosphate, and malate.[29,30,35,36] Thus, enzyme mining of thermostable A6PE and A6PP was imperative for the successful construction of this *in vitro* biosystem.

For A6PE, only one paper reported structural and functional analyses of an A6PE from *E. coli* K-12 that catalyzes the conversion of A6P and F6P.[31] This enzyme was used as a template by the Basic Local Alignment Search Tool (BLAST) for mining new thermostable A6PE. According to this study,[31] the active sites of A6PE and D-ribulose 5-phosphate 3-epimerase (RPE) are highly superimposable except for the phosphate-binding motif (positions 196, 197, and 198 of EcA6PE), which is a loop following the eighth β-strand of A6PE. This loop of EcA6PE is one residue (at position 198 of EcA6PE) longer than that of RPE. Based on this feature, we screened BLAST results and found two candidates derived from thermophilic microorganisms: TtA6PE from *T. thermosaccharolyticum* DSM 571 (UniProt Code: D9TQJ4) and TbA6PE from *T. bacterium* (UniProt Code: A0A3D6DDL0) (Table 1). Sequence alignment results showed that TtA6PE (at position S198) and TbA6PE (at position T199) both had an additional residue on the loop following the eighth β-strand and shared a highly conserved sequence motif (signature: GxSGLF) (Figure S1). This result indicated that TtA6PE and TbA6PE might have epimeric activities in converting F6P to A6P. The amino acid sequence similarity values of TtA6PE and TbA6PE to EcA6PE were 53.4 and 35.8%, respectively, and the specific activities of these two enzymes in converting F6P to A6P were 132.6 and 17.4 U/mg at 50 °C, respectively. Thus, TtA6PE with a higher specific activity was selected for the subsequent D-allulose production.

For this *in vitro* biosystem that converts starch to D-allulose, it is extremely important to find a phosphatase with high substrate specificity on A6P. Namely, this phosphatase should have high dephosphorylation activity against A6P and little activity against G1P, G6P, and F6P. Phosphatase belongs to the haloacid dehalogenase (HAD) superfamily, and members

Table 2. Screening of D-Allulose 6-Phosphate Phosphatase through Literature Mining

				specific activity (μmol/min/mg)			
abbrev.	source and its optimum growth temperature	UniProt entry number	assay temperature	D-allulose 6-phosphate	D-fructose-6-phosphate	D-glucose-6-phospate	D-glucose-1-phosphate
AcA6PP	*Acidothermus cellulolyticus* (55 °C)	A0LR15	50 °C	0.42 ± 0.05	0.15 ± 0.00	0.30 ± 0.01	0.14 ± 0.01
EcA6PP	*Escherichia coli* str. K-12 substr. MG1655 (37 °C)	P64636	37 °C	no activity	0.14 ± 0.06	0.05 ± 0.00	no activity
SaA6PP	*Streptomyces avermitilis* MA-4680 (28 °C)	Q82HY3	37 °C	no activity	no activity	no activity	no activity
BfA6PP	*Bacteroides fragilis* NCTC 9343 (37 °C)	Q5LGR4	37 °C	3.73 ± 0.30	0.82 ± 0.04	0.17 ± 0.00	no activity

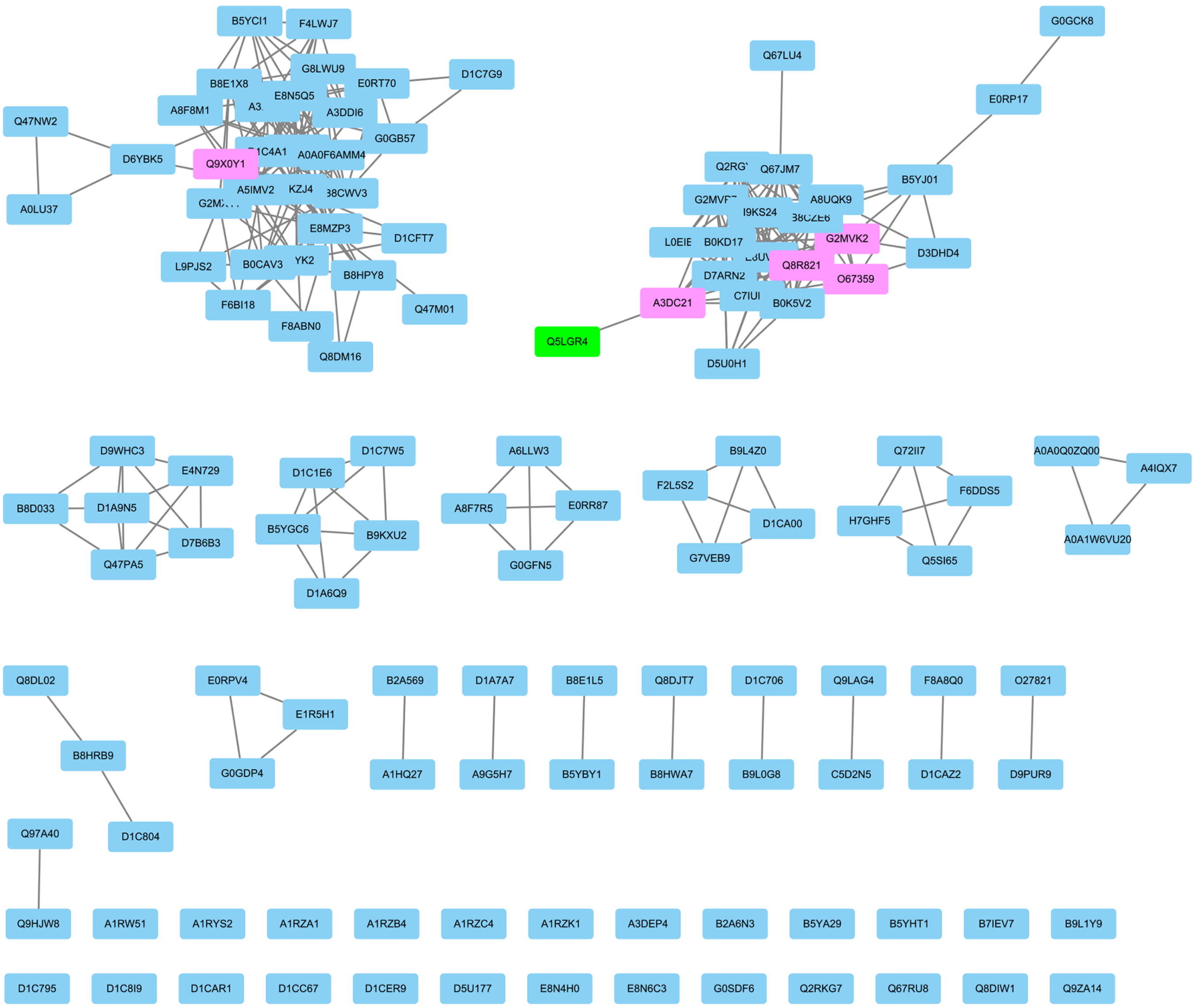

Figure 2. Sequence similarity network (SSN) generated from 129 thermophile-derived candidates with the same cap structure (C1.5.6: HAD, Beta-PGM, Phosphatase Like) as BfA6PP (Q5LGR4) and BfA6PP itself. In the network, the negative log of the *e*-value for all-by-all BLAST was set as 5, the alignment score threshold was set as 50, and the other parameters were system default values. Each node in the network represents a single protein sequence. The node of BfA6PP (Q5LGR4) is marked in green, and the proteins selected for testing the substrate specificity on sugar phosphates are marked in pink.

of this family share a rossmannoid fold "core" domain that contains the phosphoryl transfer site and a "cap" domain that provides substrate specificity.[37] In a previous study, Huang et al.[38] examined the activity profile of more than 200 HAD phosphatases by screening a customized library containing 167 sugar phosphates. From this data set, four enzyme candidates from different prokaryotic species with predicted dephosphorylation activities against A6P were chosen, and their dephosphorylation activities on G1P, G6P, F6P, and A6P were tested in this study (Table 2). Among them, the candidate from mesophilic *B. fragilis* NCTC 9343 (UniProt Code: Q5LGR4, named BfA6PP) had the best performance,

Table 3. Screening of D-Allulose 6-Phosphate Phosphatase through the Construction of SSN

abbrev.	source and its optimum growth temperature	sequence similarity with BfA6pp	UniProt entry number	assay temperature	specific activity (μmol/min/mg) D-allulose 6-phosphate	D-fructose 6-phosphate	D-glucose 6-phosphate	D-glucose 1-phosphate
CtA6PP	*Clostridium thermocellum* (60 °C)	44.7%	A3DC21	50 °C	14.25 ± 1.48	0.96 ± 0.07	0.36 ± 0.04	no activity
TmA6PP	*Thermotoga maritima* MSB8 (80 °C)	21.3%	Q9X0Y1	50 °C	no activity	1.48 ± 0.08	no activity	no activity
TwA6PP	*Thermoanaerobacter wiegelii* (65 °C)	28.8%	G2MVK2	50 °C	no activity	0.36 ± 0.02	no activity	no activity
AaA6PP	*Aquifex aeolicus* (95 °C)	22.1%	O67359	60 °C	no activity	0.06 ± 0.01	0.02 ± 0.01	0.02 ± 0.01
CsA6PP	*Caldanaerobacter subterraneus* (70 °C)	26.4%	Q8R821	50 °C	no activity	0.29 ± 0.01	0.19 ± 0.01	no activity

and its specific activity against A6P was 3.7 U/mg at 37 °C, which was 4.5- and 21.9-fold higher than those of F6P and G6P, respectively, and it had no activity against G1P. However, BfA6PP is not a thermophilic enzyme and cannot be compatible with other thermophilic enzymes used in this biosystem in one pot because of its low thermostability. Thus, a thermophilic A6PP was highly required. Enzymes in the haloacid dehalogenase superfamily were collected and summarized in the Structure−Function Linkage Database (SFLD) (http://sfld.rbvi.ucsf.edu/archive/django/superfamily/3/index.html);[37] moreover, we exported the database and obtained a total of 129 thermophile-derived candidates with the same cap structure (C1.5.6: HAD, Beta-PGM, Phosphatase Like) as BfA6PP (Supporting Information S2). Then, a sequence similarity network (SSN), which is a visually powerful tool for analyzing sequence relationships in protein families,[39] was constructed using 129 thermophile-derived candidates and BfA6PP (Figure 2). The nodes of this SSN were marked using the UniProt Code. In this SSN, the node representing BfA6PP (Q5LGR4) was marked in green. As shown in Figure 2, the protein A3DC21 (derived from *Clostridium thermocellum*, named CtA6PP) had the closest relationship with BfA6PP (Q5LGR4). *C. thermocellum* is a thermophilic microorganism, and the dephosphorylation activities of A3DC21 on G1P, G6P, F6P, and A6P were checked. As shown in Table 3, CtA6PP showed the desired substrate preference in the *in vitro* biosystem for converting starch to D-allulose. Its specific activity against A6P was 14.3 U/mg at 50 °C, which was 14.8- and 39.6-fold higher than those of F6P and G6P, respectively, and it had no activity against G1P. In addition, the sequences of all the candidates from thermophilic microorganisms in this SSN and BfA6PP were aligned, and the other four enzymes (Q9X0Y1, G2MVK2, O67359, and Q8R821) with relatively high sequence similarity with BfA6PP were also tested (Table 3). These four enzymes along with CtA6PP are marked in pink in Figure 2, three of which were in the same cluster as BfA6PP and CtA6PP in the SSN. However, none of these four thermophilic enzymes showed dephosphorylation activity on A6P. Thus, thermophilic CtA6PP was selected for the subsequent D-allulose production.

Validation and Optimization of One-Pot Biosynthesis of D-Allulose. Before the proof-of-concept experiment, the concentrations of glucose, fructose, and D-allulose were detected by HPLC equipped with a Bio-Rad HPX-87H column using 5 mM H_2SO_4 as a mobile phase and a refractive index detector. The retention time values of glucose, fructose, and D-allulose were 9.0, 9.7, and 10.1 min (Figure S2A), respectively, indicating that these chemical compounds can be distinguished by HPLC. The peak intensities had linear relationships with certain concentration ranges of glucose (Figure S2B), fructose (Figure S2C), and D-allulose (Figure S2D), indicating that these compounds can be quantified by this method.

For the proof-of-concept experiment, all the enzymes were purified by simple heat treatment, and the purities of the recombinant proteins were checked by 12% SDS-PAGE (Figure S3). Before the proof-of-concept experiment, the maltodextrin substrate (DE = 4−7) was pretreated with IA at 80 °C for 2.5 h with a substrate-to-enzyme mass ratio of 1500:1. Then, the reaction for the production of D-allulose was conducted in 10 mM sodium phosphate buffer (pH 7.5) containing 5 mM $MgCl_2$, 10 g/L IA-treated maltodextrin (55 mM glucose equivalent), and 2.0 U/mL of TmαGP, TkPGM, TtcPGI, TtA6PE, and CtA6PP at 50 °C for 24 h. At different time points, a part of the reaction solution was subjected to HPLC for detection. As shown in Figure 3A, the HPLC peak height of D-allulose increased over time until 12 h, indicating the feasibility of synthesizing D-allulose from starch by this *in vitro* biosystem. However, the by-products fructose and glucose also appeared. After the reaction had proceeded for 24 h, the concentrations of D-allulose, fructose, and glucose were 23.0, 1.9, and 1.3 mM, respectively (Figure 3B). The product yield of D-allulose based on the initial 55 mM glucose equivalent maltodextrin was 41.9%. Because the yield of D-allulose was much lower than the theoretical value, the reaction conditions, including the buffer pH, reaction temperature, and enzyme loading amounts, were optimized. As shown in Figure S4, the optimal pH and temperature for D-allulose production were 7.0 and 55 °C, respectively.

Enzyme loading amounts of each enzyme were crucial for high product yield by the *in vitro* biosystem; thus, the enzyme loading amounts of our *in vitro* biosystem were optimized one by one under the optimum pH and reaction temperature using an *in vitro* titration method as described before.[30] When the initial concentration of IA-treated maltodextrin was 10 g/L, the concentration of TmαGP was changed from 0.5 to 5.0 U/mL while the other four enzyme loadings were 2.0 U/mL each. The productivity of D-allulose rapidly increased from 1.9 to 5.5 mM/h when the concentration of TmαGP was increased from 0.5 to 2.0 U/mL (Figure 4A). When the concentration of TmαGP was more than 2.0 U/mL, there was only a slow increase in the productivity of D-allulose. Therefore, the optimal TmαGP loading was set at 2 U/mL, and it was used for the subsequent optimization of the other enzyme loadings. Finally, the optimal enzyme loadings of TmαGP, TkPGM, TtcPGI, TtA6PE, and CtA6PP were 2.0 (Figure 4A), 0.5 (Figure 4B), 0.5 (Figure 4C), 2.0 (Figure 4D), and 3.0 U/mL

https://doi.org/10.1021/acscatal.0c05718
ACS Catal. 2021, 11, 5088−5099

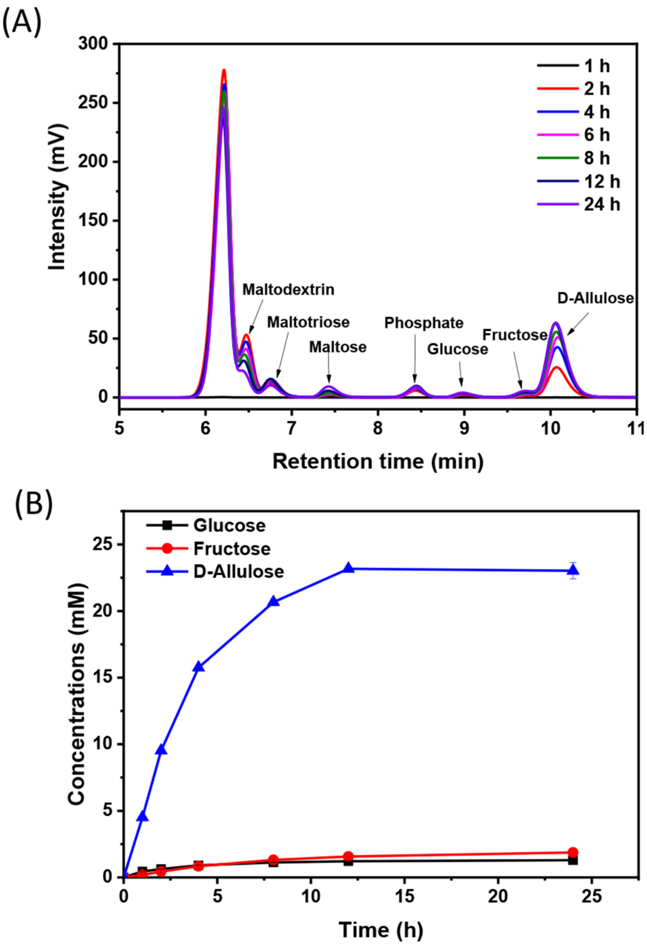

Figure 3. Proof-of-concept production of D-allulose from IA-treated maltodextrin by the five core enzymes. (A) HPLC chromatograms of the peaks of D-allulose, fructose, glucose, phosphate, maltose, maltotriose, and maltodextrin at different time points. (B) Time profiles of glucose (square), fructose (circle), and D-allulose (triangle) in the system for the proof-of-concept production of D-allulose from IA-treated maltodextrin by the five core enzymes. The experiment was carried out in 10 mM sodium phosphate buffer (pH 7.5) containing 10 mM $MgCl_2$, IA-treated maltodextrin (10 g/L, 55 mM glucose equivalent), and 2 U/mL of each enzyme for 24 h at 50 °C. Values shown are the means of triplicate determinations.

(Figure 4E), respectively, for converting 10 g/L IA-treated maltodextrin to D-allulose.

Then, D-allulose was produced under the optimal conditions, and the reaction was performed at 55 °C in 10 mM sodium phosphate buffer (pH 7.0) containing 5 mM $MgCl_2$, 10 g/L IA-treated maltodextrin (55 mM glucose equivalent), 2.0 U/mL TmαGP, 0.5 U/mL TkPGM, 0.5 U/mL TtcPGI, 2.0 U/mL TtA6PE, and 3.0 U/mL CtA6PP. The reaction rate for D-allulose production was 6.8 mM/h for the first 4 h, which was two times higher than that in the proof-of-concept reaction. The final concentration and yield of D-allulose after reaction for 24 h were 34.1 mM and 62.0%, respectively, which were 1.5 times higher than that of the proof-of-concept reaction (Figure 5). In addition, the concentrations of by-products fructose and glucose were 4.4 and 2.0 mM, accounting for 7.9 and 3.6% conversion yields, respectively. The remaining unused substrates accounted for 26.4%, mainly containing maltobiose and maltotriose (Figure S5). In addition, maltotriose continued to decrease in the late phase of the reaction while substantial concentrations of maltose accumulated, indicating that the easily available substrate of TmαGP was exhausted.

To achieve the complete utilization of maltodextrin for D-allulose production, three auxiliary enzymes, including 4-α-glucanotransferase (4GT) from *Thermococcus litoralis* DSM 5473, polyphosphate glucokinase (PPGK) from *Thermobifida fusca* YX, and glucose isomerase (GI) purchased from Novozymes, were added to the reaction (Table S1 and Figure 6A). 4GT was used to rearrange one anhydroglucose unit from maltose/maltotriose to another maltose/maltotriose to yield a short-chain amylodextrin by releasing one glucose molecule. After the conversion of 10 g/L IA-treated maltodextrins to D-allulose under optimal conditions for 6 h, 2.0 U/mL 4GT was added into the reaction solution, resulting in a final concentration of D-allulose of 39.4 mM, with a product yield of 69.9%. To utilize the residual glucose molecules released by 4GT, PPGK and polyphosphate were added to convert glucose to G6P; thus, the final concentration of D-allulose was increased to 45.0 mM, with a product yield of 81.8%. Meanwhile, the concentration of the by-product fructose was 9.1 mM, and then GI was added to convert fructose to glucose, which was further utilized by PPGK to generate G6P. After GI was added into the system, the D-allulose titer was increased to 48.5 mM, which was 88.2% of the theoretical maximum yield. However, fructose cannot be utilized completely and remained at approximately 5.3 mM in the final solution (Figure 6B). At the same time, the amount of polyphosphate added in the reaction was optimized, excess concentrations (8 and 12 mM) of polyphosphate were used, and no significant difference was seen in the product yield of D-allulose (Table S2).

D-Allulose Production from High Concentrations of Maltodextrin. To investigate the potential application of this *in vitro* synthetic enzymatic biosystem for the production of D-allulose on an industrial scale, the substrate IA-treated maltodextrin concentration was set at 275 mM glucose equivalent (50 g/L). As the concentration of maltodextrin was 5-fold that in the previously optimized biosystem, the enzyme loadings were also increased by 5-fold. When only five core enzymes were used for the reaction, the production of D-allulose reached a maximum of 131.6 mM at 4 h and then slowly decreased. The concentration of fructose increased from 26.4 mM at 4 h to 96.0 mM at 24 h (Figure 7A). After three auxiliary enzymes (4GT, PPGK, and GI) and polyphosphate were added at 5 h, the production of D-allulose continued to increase while the production of fructose was significantly suppressed. After 24 h, the final D-allulose concentration was 217.8 mM with a product yield of 79.2% based on the initial maltodextrin (Figure 7B) while the final concentration values of fructose and glucose were 26.6 and 19.7 mM, respectively. Similarly, no significant difference was also seen in the final yield of D-allulose when 40 or 60 mM polyphosphate was used (Table S2).

■ DISCUSSION

In this study, we developed an *in vitro* enzymatic pathway for the synthesis of D-allulose from starch. Through mining thermostable enzymes A6PP and A6PE, optimizing the reaction conditions (including the buffer pH, reaction temperature, and enzyme loading amounts), and adding four auxiliary enzymes (IA, 4GT, PPGK, and GI), 48.5 and 217.8 mM D-allulose were produced, which represented yields of 88.2 and 79.2% from 10 and 50 g/L maltodextrin, respectively. This study provides a good example of a "design-build-test-analysis

https://doi.org/10.1021/acscatal.0c05718
ACS Catal. 2021, 11, 5088−5099

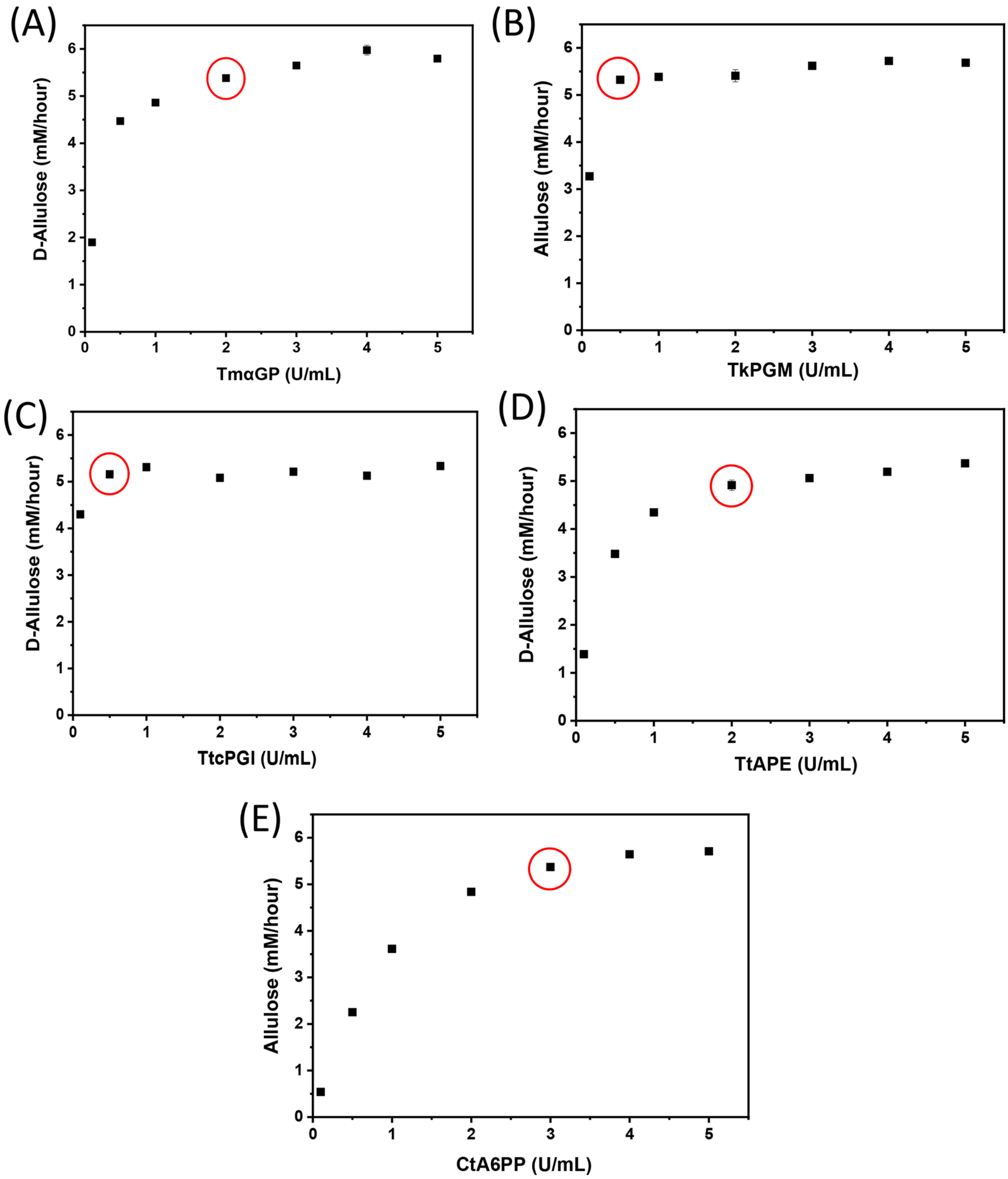

Figure 4. Optimization of enzyme loading amounts for D-allulose production from 10 g/L IA-treated maltodextrin. The reaction was performed at 55 °C in 10 mM sodium phosphate buffer (pH 7.0), 5 mM $MgCl_2$, IA-treated maltodextrin (10 g/L, 55 mM glucose equivalent) plus a five-enzyme cocktail for 4 h. (A) Effect of TmαGP concentration from 0.1 to 5.0 U/mL in the presence of 2.0 U/mL TkPGM, 2.0 U/mL TtcPGI, 2.0 U/mL TtA6PE, and 2.0 U/mL CtA6PP. (B) Effect of TkPGM concentration from 0.1 to 5.0 U/mL in the presence of 2.0 U/mL TmαGP, 2.0 U/mL TtcPGI, 2.0 U/mL TtA6PE, and 2.0 U/mL CtA6PP. (C) Effect of TtcPGI concentrations from 0.1 to 5.0 U/mL in the presence of 2.0 U/mL TmαGP, 0.5 U/mL TkPGM, 2.0 U/mL TtA6PE, and 2.0 U/mL CtA6PP. (D) Effect of TtA6PE concentration from 0.1 to 5.0 U/mL in the presence of 2.0 U/mL TmαGP P, 0.5 U/mL TkPGM, 0.5 U/mL TtcPGI, and 2.0 U/mL CtA6PP. (E) Effect of CtA6PP concentration from 0.1 to 5.0 U/mL in the presence of 2.0 U/mL TmαGP, 0.5 U/mL TkPGM, 0.5 U/mL TtcPGI, and 2.0 U/mL TtA6PE. The circled concentration values were considered the optimal concentrations. Values shown are the means of triplicate determinations.

cycle" to obtain a high yield of D-allulose production from starch, thus demonstrating the great engineering flexibility of *in vitro* synthetic enzymatic biosystems.

Compared to the traditional enzymatic epimerization method, this *in vitro* biosystem for D-allulose production has the following advantages for cost-saving: (1) the raw material starch is much cheaper than pure fructose, which is mainly produced from starch by an enzymatic method followed by careful separation; (2) a much higher production yield of D-allulose can be obtained due to the last irreversible dephosphorylation step; and (3) because of the high product yield of D-allulose, the product separation and purification processes are simplified, avoiding investing in expensive equipment (for example, simulated moving bed chromatography) to obtain high-purity products. Herein, note that the number of enzymes used in this study was more than that for

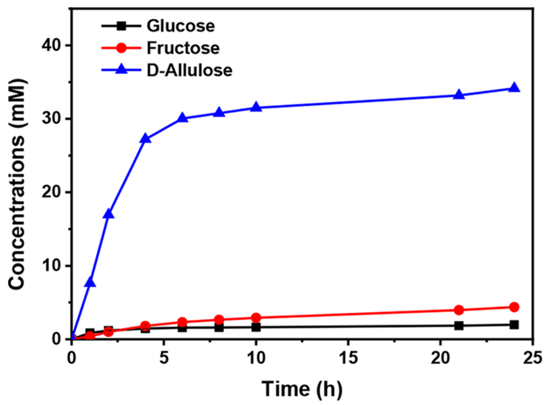

Figure 5. Time profile of D-allulose production from maltodextrin under the optimized reaction conditions. The reaction was performed at 55 °C in 10 mM sodium phosphate buffer (pH 7.0), 5 mM $MgCl_2$, IA-treated maltodextrin (10 g/L, 55 mM glucose equivalent), and 2.0 U/mL TmαGP, 0.5 U/mL TkPGM, 0.5 U/mL TtcPGI, 2.0 U/mL TtA6PE, and 3.0 U/mL CtA6PP for 24 h. Values shown are the means of triplicate determinations.

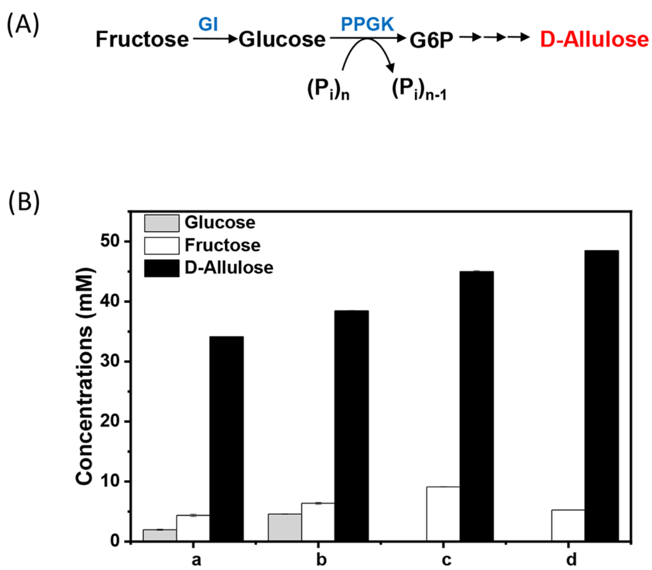

Figure 6. Schematic representation of the enzymatic pathway for converting fructose to D-allulose (A) and concentrations of D-allulose, fructose, and glucose produced from 55 mM glucose-equivalent IA-treated maltodextrin (10 g/L) under the optimized reaction conditions (B). The reaction was catalyzed by a five-enzyme cocktail (5E) (a), a five-enzyme cocktail with 4GT (5E + 4GT) (b), a five-enzyme cocktail with 4GT and PPGK (5E + 4GT + PPGK) (c), and a five-enzyme cocktail with 4GT, PPGK, and GI (5E + 4GT + PPGK + GI) (d). Values shown are the means of triplicate determinations.

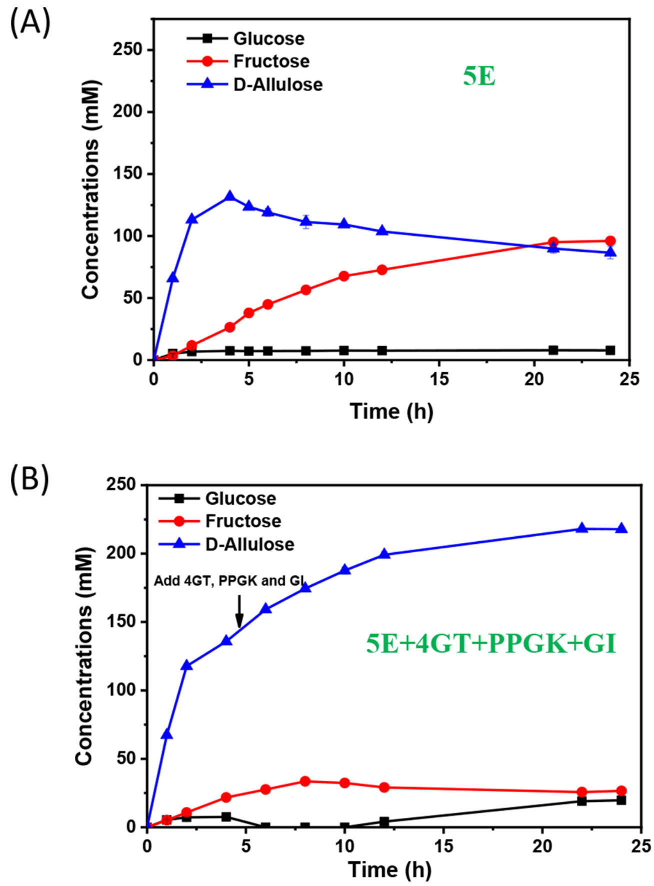

Figure 7. D-Allulose synthesis profile from IA-treated maltodextrin (50 g/L, 275 mM glucose equivalent) catalyzed by a five-enzyme cocktail without (A) or with (B) auxiliary enzymes (4GT, PPGK, and GI). The reaction was carried out in 30 mM sodium phosphate buffer (pH 7.0) at 55 °C containing 5 mM $MgCl_2$, 50 g/L IA-treated maltodextrin (275 mM glucose equivalent), 10.0 U/mL TmαGP, 2.5 U/mL TkPGM, 2.5 U/mL TtcPGI, 10.0 U/mL TtA6PE, and 15.0 U/mL CtA6PP for 24 h. After reaction for 5 h, 10.0 U/mL Tl4GT, 10.0 U/mL TfuPPGK, 10.0 U/mL GI, 60 mM polyphosphate, and 60 mM $MgCl_2$ were added to the reaction solution. Values shown are the means of triplicate determinations.

the traditional enzymatic epimerization method for D-allulose production, and it may increase the enzyme cost for our D-allulose production. However, enzyme cost could be significantly decreased or even negligible by finding better enzymes combined with enzyme immobilization.[40]

During D-allulose production by this *in vitro* biosystem, the product yields are dependent on the DP value of the maltodextrin. When using DE 4−7 maltodextrin as a substrate, the measured DP value of IA-treated maltodextrin was about 11 according to a previously described method.[41] Since αGP has no activity on maltose, if the five core enzymes are used for the D-allulose conversion, the products are maltose and D-allulose without any side reactions. The yields of D-allulose and maltose are 81.8 (9/11) and 18.2% (2/11), respectively, and no glucose will produce in theory. When 4GT is further added to the reaction, every two molecules of maltose will produce one molecule of glucose and one molecule of maltotriose, where maltotriose can be utilized by αGP to generate maltose and glucose. Thus, the yield of glucose should be no more than 9.1% (1/11). PPGK and polyphosphate could convert glucose to G6P, all the glucose units in the maltodextrin could be converted to D-allulose with a theoretical yield of 100%, and no glucose should be in the reaction system in theory. However, some glucose remained in the biosystem using the high concentration of maltodextrin in the later reaction stage, and this result might be due to the inactivation of PPGK because of the accumulation of phosphate ions or the weak thermo-stability of PPGK. Because CtA6PP had catalytic activity on G6P in our *in vitro* biosystem, the promiscuous activity of CtA6PP on G6P and the action of 4GT both contributed to the accumulation of glucose (Figure 7B). The concentration of fructose production was higher than that of glucose (Figures 5 and 7A), especially in the situation of a high concentration of substrate (Figure 7A). This result cannot be simply explained by the specific activity of CtA6PP on F6P being higher than that of G6P. A6PE has been reported to employ a deprotonation/reprotonation mechanism using an acid and base catalyst and can be classified into Family Three of Carbohydrate Epimerases.[42] Members of this family may be active both on phosphate sugars and monosaccharide substrates.[42] In this study, we determined whether TtA6PE had monosaccharide epimerization activity. The results showed that TtA6PE not only catalyzed the interconversion of F6P and A6P but also catalyzed the interconversion of D-allulose and fructose (Figure S6A). TbA6PE (Figure S6B) and EcA6PE (Figure S6C) also had the same function as TtA6PE. The K_m value of TtA6PE was more than 2.0 mol/L D-allulose (Figure S6D), which was too high to measure a specific value. The monosaccharide epimerization activity of TtA6PE was very low at low concentrations of D-allulose but increased as the concentration of D-allulose increased. This result could explain the fructose concentration in Figures 5 and 7A. When the initial concentration of maltodextrin was 10 g/L, only ~30 mM D-allulose was generated. Under this situation, TtA6PE catalyzed undetectable monosaccharide epimerization that converted D-allulose to fructose, resulting in an unperceivable increase in fructose (Figure 5). When the initial concentration of maltodextrin was increased by 5-fold, a higher concentration of D-allulose accumulated and the epimerization activity of TtA6PE also increased, resulting in an increased concentration of fructose and a decreased concentration of D-allulose (Figure 7A). Because the catalytic activity of TtA6PE on converting F6P to A6P was much higher than that of converting D-allulose to fructose, after three auxiliary enzymes (4GT, PPGK, and GI) were added into the reaction solution, the generation rate of D-allulose from fructose through the enzymatic pathway listed in Figure 6A was much higher than fructose generation from the epimerization of D-allulose, resulting in the continuous increase of D-allulose from the high concentration of maltodextrin (Figure 7B).

The timing for the addition of auxiliary enzymes (4GT, PPGK, and GI) was chosen based on the appearance of their substrates in the biosystem. αGP, which was responsible for the phosphorylation of dextrin, has no or little activity on maltose and maltotriose. The function of 4GT was to polymerize the maltose and maltotriose to the relative long-chain dextrin for the utilization of αGP, releasing glucose finally. Meanwhile, 4GT could also catalyze the cyclization of long-chain dextrin,[43] and cyclized dextrin could not be utilized by αGP to produce G1P. Thus, 4GT must be added at the time when the long-chain dextrin was almost exhausted to avoid affecting the product yield. This time was 6 (the initial maltodextrin was 55 mM) or 5 h (the initial maltodextrin was 275 mM) when the reaction rate of the whole system began to decrease (Figures 3B and 7A). The substrates of PPGK were polyphosphate and glucose, and glucose was the product of 4GT and the side product of A6PP. The substrate of GI was fructose, which was the side product of A6PE and A6PP, and GI catalyzed fructose to glucose. Thus, PPGK, polyphosphate, and GI should be better added with 4GT at the same time. Because glucose and fructose appeared early in the current biosystem, PPGK, polyphosphate, and GI could also be added at the beginning of the reaction. If A6PE and A6PP with high substrate specificities were found, GI could be omitted because no fructose will be generated. Meanwhile, the usage of PPGK and polyphosphate can also be significantly decreased because only 4GT could generate glucose, whose concentration should be at a low level. The reduction of polyphosphate can not only reduce the cost of raw materials but also facilitate the separation and purification of products and related wastewater treatment processes.

To further increase D-allulose production efficiency from maltodextrin based on this "thermodynamics-driven cascade reaction" route, several issues need to be considered: (1) Gene mining and protein engineering for better enzymes, especially for A6PE and A6PP. In this study, SSN was used to obtain potential natural enzymes; however, the accuracy to find the desired enzymes by SSN was highly dependent on the current databases and the properties of natural enzymes cannot meet the requirement of industrial application in most circumstances. Protein engineering methods such as directed evolution[44−46] might be an alternative to obtaining A6PE and A6PP with higher catalytic activities, better thermostability, and substrate specificity. (2) Enzyme immobilization for higher system stability. Immobilization techniques are known to increase enzyme thermostability and allow for quick separation of the enzyme from the reaction solution, thereby stimulating the industrial application of biocatalysts. Adsorption, entrapment, and cross-linking are the most widely used enzyme immobilization methods, and we plan to co-immobilize the enzymes by these methods in combination with emerging nanomaterials, such as metal−organic or covalent organic frameworks (MOFs and COFs),[47] carboxyl-functionalized graphene oxide,[48] and polymeric nanoparticles.[49] In addition, enzyme immobilization using the cross-linked enzyme aggregate (CLEA) technique coupled with magnetic particles,[50] which combines enzyme purification and immobilization into a single unit operation, is also a good choice. (3) Build stoichiometric mathematical models for quick optimization. In this study, the enzyme ratio was optimized by the method of titration experiment. Using the mathematical model based on the catalytic mechanisms and kinetic parameters of enzymes could provide a rapid and precise method to obtain the optimal reaction condition.[51] However, the undesired reactions catalyzed by TtA6PE and CtA6PP bring difficulty and complexity to build a precise mathematical model to simulate the reaction process of the *in vitro* biosystem. When the A6PE and A6PP with high substrate specificities were obtained by gene mining or protein engineering, the mathematic model could be built to find the optimal conditions quickly for decreasing the production cost of D-allulose.

In conclusion, we demonstrated the one-pot biosynthesis of D-allulose from starch *via* an *in vitro* synthetic enzymatic biosystem using several thermophilic enzymes. This *in vitro* biosystem is cofactor-free. Approximately 48.5 and 217.8 mM D-allulose with product yields of 88.2 and 79.2% were produced from 10 and 50 g/L maltodextrin, respectively. These product yields of D-allulose were much higher than those of the traditional Izumoring epimerization method. So, the proposed system provides a cost-efficient route for the biomanufacture of D-allulose. This strategy of a thermodynamics-driven phosphorylation-dephosphorylation cascade reaction may provide a revolutionary method for producing rare sugars (tagatose, mannitol, sorbitol, *etc.*) from inexpensive starch. Future work will include gene mining, protein engineering, enzyme co-immobilization, and industrial process optimization.

https://doi.org/10.1021/acscatal.0c05718
ACS Catal. 2021, 11, 5088−5099

ASSOCIATED CONTENT

Supporting Information

The Supporting Information is available free of charge at https://pubs.acs.org/doi/10.1021/acscatal.0c05718.

Table S1−S2, Figure S1−S6 (PDF)

Haloacid dehalogenase family and filters (XLSX)

AUTHOR INFORMATION

Corresponding Author

Chun You − *Tianjin Institute of Industrial Biotechnology, Chinese Academy of Sciences, Tianjin 300308, China; National Technology Innovation Center of Synthetic Biology, Tianjin 300308, China; University of Chinese Academy of Sciences, Beijing 100049, People's Republic of China;* orcid.org/0000-0003-2305-336X; Email: you_c@tib.cas.cn

Authors

Yunjie Li − *Tianjin Institute of Industrial Biotechnology, Chinese Academy of Sciences, Tianjin 300308, China; National Technology Innovation Center of Synthetic Biology, Tianjin 300308, China;* orcid.org/0000-0002-4464-1470

Ting Shi − *Tianjin Institute of Industrial Biotechnology, Chinese Academy of Sciences, Tianjin 300308, China; National Technology Innovation Center of Synthetic Biology, Tianjin 300308, China*

Pingping Han − *Tianjin Institute of Industrial Biotechnology, Chinese Academy of Sciences, Tianjin 300308, China; National Technology Innovation Center of Synthetic Biology, Tianjin 300308, China*

Complete contact information is available at: https://pubs.acs.org/10.1021/acscatal.0c05718

Author Contributions

[&]Y.L. and T.S. are equal contributors. Y.L., T.S., and C.Y. designed experiments and analyzed the data. Y.L., T.S., P.H., and C.Y. drafted the manuscript. Y.L. and T.S. performed the experiments. All authors discussed the results and commented on the manuscript.

Notes

The authors declare no competing financial interest.

ACKNOWLEDGMENTS

This work was supported by the National Natural Science Foundation of China (Grant No. 31600635, 31700033, 21778073, and 32022044), the High-tech Innovation Fund of the Chinese Academy of Sciences (GQRC-19-11), the Biological Resources Program of the Chinese Academy of Sciences (No. KFJ-BRP-009), and the Tianjin Synthetic Biotechnology Innovation Capacity Improvement Project (TSBICIP-KJGG-003).

REFERENCES

(1) Hossain, A.; Yamaguchi, F.; Matsuo, T.; Tsukamoto, I.; Toyoda, Y.; Ogawa, M.; Nagata, Y.; Tokuda, M. Rare Sugar D-Allulose: Potential Role and Therapeutic Monitoring in Maintaining Obesity and Type 2 Diabetes Mellitus. *Pharmacol. Ther.* **2015**, *155*, 49−59.

(2) Chattopadhyay, S.; Raychaudhuri, U.; Chakraborty, R. Artificial Sweeteners-a Review. *J. Food Sci. Technol.* **2014**, *51*, 611−621.

(3) Mooradian, A. D.; Smith, M.; Tokuda, M. The Role of Artificial and Natural Sweeteners in Reducing the Consumption of Table Sugar: A Narrative Review. *Clin. Nutr. ESPEN.* **2017**, *18*, 1−8.

(4) Edwards, C. H.; Rossi, M.; Corpe, C. P.; Butterworth, P. J.; Ellis, P. R. The Role of Sugars and Sweeteners in Food, Diet and Health: Alternatives for the Future. *Trends Food Sci. Technol.* **2016**, *56*, 158−166.

(5) Zhang, W.; Yu, S.; Zhang, T.; Jiang, B.; Mu, W. Recent Advances in D-Allulose: Physiological Functionalities, Applications, and Biological Production. *Trends Food Sci. Technol.* **2016**, *54*, 127−137.

(6) Zhang, W.; Zhang, T.; Jiang, B.; Mu, W. Enzymatic Approaches to Rare Sugar Production. *Biotechnol. Adv.* **2017**, *35*, 267−274.

(7) Beerens, K.; Van Overtveldt, S.; Desmet, T. The "Epimerring" Highlights the Potential of Carbohydrate Epimerases for Rare Sugar Production. *Biocatal. Biotransform.* **2017**, *35*, 230−237.

(8) Ayers, B. J.; Hollinshead, J.; Saville, A. W.; Nakagawa, S.; Adachi, I.; Kato, A.; Izumori, K.; Bartholomew, B.; Fleet, G. W. J.; Nash, R. J. Iteamine, the First Alkaloid Isolated from Itea Virginica L. Inflorescence. *Phytochemistry* **2014**, *100*, 126−131.

(9) Miller, B. S.; Swain, T. Chromatographic Analyses of the Free Amino-Acids, Organic Acids and Sugars in Wheat Plant Extracts. *J. Sci. Food Agric.* **1960**, *11*, 344−348.

(10) Oshima, H.; Kimura, I.; Zumori, K. Psicose Contents in Various Food Products and Its Origin. *Food Sci. Technol. Res.* **2006**, *12*, 137−143.

(11) Matsuo, T.; Suzuki, H.; Hashiguchi, M.; Izumori, K. D-Psicose Is a Rare Sugar That Provides No Energy to Growing Rats. *J. Nutr. Sci. Vitaminol.* **2002**, *48*, 77−80.

(12) Matsuo, T.; Baba, Y.; Hashiguchi, M.; Takeshita, K.; Izumori, K.; Suzuki, H. Dietary D-Psicose, a C-3 Epimer of D-Fructose, Suppresses the Activity of Hepatic Lipogenic Enzymes in Rats. *Asia Pac. J. Clin. Nutr.* **2001**, *10*, 233−237.

(13) Hayashi, N.; Iida, T.; Yamada, T.; Okuma, K.; Takehara, I.; Yamamoto, T.; Yamada, K.; Tokuda, M. Study on the Postprandial Blood Glucose Suppression Effect of D-Psicose in Borderline Diabetes and the Safety of Long-Term Ingestion by Normal Human Subjects. *Biosci., Biotechnol., Biochem.* **2010**, *74*, 510−519.

(14) Chung, M. Y.; Oh, D. K.; Lee, K. W. Hypoglycemic Health Benefits of D-Psicose. *J. Agric. Food Chem.* **2012**, *60*, 863−869.

(15) Moller, D. E.; Berger, J. P. Role of PPARs in the Regulation of Obesity-Related Insulin Sensitivity and Inflammation. *Int. J. Obes. Relat. Metab. Disord.* **2003**, *27*, 17−21.

(16) Takata, M. K.; Yamaguchi, F.; Nakanose, K.; Watanabe, Y.; Hatano, N.; Tsukamoto, I.; Nagata, M.; Izumori, K.; Tokuda, M. Neuroprotective Effect of D-Psicose on 6-Hydroxydopamine-Induced Apoptosis in Rat Pheochromocytoma (PC12) Cells. *J. Biosci. Bioeng.* **2005**, *100*, 511−516.

(17) Suna, S.; Yamaguchi, F.; Kimura, S.; Tokuda, M.; Jitsunari, F. Preventive Effect of D-Psicose, One of Rare Ketohexoses, on Di-(2-Ethylhexyl) Phthalate (DEHP)-Induced Testicular Injury in Rat. *Toxicol. Lett.* **2007**, *173*, 107−117.

(18) Murao, K.; Yu, X.; Cao, W. M.; Imachi, H.; Chen, K.; Muraoka, T.; Kitanaka, N.; Li, J.; Ahmed, R. A. M.; Matsumoto, K.; Nishiuchi, T.; Tokuda, M.; Ishida, T. D-Psicose Inhibits the Expression of MCP-1 Induced by High-Glucose Stimulation in Huvecs. *Life Sci.* **2007**, *81*, 592−599.

(19) Zeng, Y.; Zhang, X.; Guan, Y.; Sun, Y. Characteristics and Antioxidant Activity of Maillard Reaction Products from Psicose-Lysine and Fructose-Lysine Model Systems. *J. Food Sci.* **2011**, *76*, C398−C403.

(20) Mcdonald, E. J. A New Synthesis of D-Psicose (D-Ribo-Hexulose). *Carbohydr. Res.* **1967**, *5*, 106−108.

(21) Doner, L. W. Isomerization of D-Fructose by Base: Liquid-Chromatographic Evaluation and the Isolation of D-Psicose. *Carbohydr. Res.* **1979**, *70*, 209−216.

(22) Granström, T. B.; Takata, G.; Tokuda, M.; Izumori, K. Izumoring: A Novel and Complete Strategy for Bioproduction of Rare Sugars. *J. Biosci. Bioeng.* **2004**, *97*, 89−94.

(23) Ekeberg, D.; Morgenlie, S.; Stenstrøm, Y. Aldose-Ketose Interconversion in Pyridine in the Presence of Aluminium Oxide. *Carbohydr. Res.* **2007**, *342*, 1992−1997.
(24) Kim, N. H.; Kim, H. J.; Kang, D. I.; Jeong, K. W.; Lee, J. K.; Kim, Y.; Oh, D. K. Conversion Shift of D-Fructose to D-Psicose for Enzyme-Catalyzed Epimerization by Addition of Borate. *Appl. Environ. Microbiol.* **2008**, *74*, 3008−3013.
(25) van Duc Long, N.; Le, T. H.; Kim, J. I.; Lee, J. W.; Koo, Y. M. Separation of D-Psicose and D-Fructose Using Simulated Moving Bed Chromatography. *J. Sep. Sci.* **2009**, *32*, 1987−1995.
(26) Li, C.; Lin, J.; Guo, Q.; Zhang, C.; Du, K.; Lin, H.; Lin, J. D-Psicose 3-Epimerase Secretory Overexpression, Immobilization, and D-Psicose Biotransformation, Separation and Crystallization. *J. Chem. Technol. Biotechnol.* **2018**, *93*, 350−357.
(27) Shi, T.; Han, P.; You, C.; Zhang, Y.-H. P. J. An *in vitro* Synthetic Biology Platform for Emerging Industrial Biomanufacturing: Bottom-up Pathway Design. *Synth. Syst. Biotechnol.* **2018**, *3*, 186−195.
(28) Yang, J.; Zhang, T.; Tian, C.; Zhu, Y.; Zeng, Y.; Men, Y.; Chen, P.; Sun, Y.; Ma, Y. Multi-Enzyme Systems and Recombinant Cells for Synthesis of Valuable Saccharides: Advances and Perspectives. *Biotechnol. Adv.* **2019**, *37*, 107406.
(29) You, C.; Shi, T.; Li, Y.; Han, P.; Zhou, X.; Zhang, Y.-H. P. An *in vitro* Synthetic Biology Platform for the Industrial Biomanufacturing of *Myo*-Inositol from Starch. *Biotechnol. Bioeng.* **2017**, *114*, 1855−1864.
(30) Wang, W.; Liu, M.; You, C.; Li, Z.; Zhang, Y.-H. P. ATP-Free Biosynthesis of a High-Energy Phosphate Metabolite Fructose 1,6-Diphosphate by *in vitro* Metabolic Engineering. *Metab. Eng.* **2017**, *42*, 168−174.
(31) Chan, K. K.; Fedorov, A. A.; Fedorov, E. V.; Almo, S. C.; Gerlt, J. A. Structural Basis for Substrate Specificity in Phosphate Binding (Beta/Alpha)$_8$-Barrels: D-Allulose 6-Phosphate 3-Epimerase from *Escherichia Coli* K-12. *Biochemistry* **2008**, *47*, 9608−9617.
(32) Saheki, S.; Takeda, A.; Shimazu, T. Assay of Inorganic Phosphate in the Mild pH Range, Suitable for Measurement of Glycogen Phosphorylase Activity. *Anal. Biochem.* **1985**, *148*, 277−281.
(33) Kim, J. E.; Kim, E. J.; Chen, H.; Wu, C. H.; Adams, M. W. W.; Zhang, Y.-H. P. Advanced Water Splitting for Green Hydrogen Gas Production through Complete Oxidation of Starch by *in vitro* Metabolic Engineering. *Metab. Eng.* **2017**, *44*, 246−252.
(34) You, C.; Zhang, Y.-H. P. Biomanufacturing by *in vitro* Biosystems Containing Complex Enzyme Mixtures. *Process Biochem.* **2017**, *52*, 106−114.
(35) Sun, S.; Wei, X.; You, C. The Construction of an *in vitro* Synthetic Enzymatic Biosystem That Facilitates Laminaribiose Biosynthesis from Maltodextrin and Glucose. *Biotechnol. J.* **2019**, *14*, No. e1800493.
(36) Shi, T.; Liu, S.; Zhang, Y.-H. P. J. CO_2 Fixation for Malate Synthesis Energized by Starch *via in vitro* Metabolic Engineering. *Metab. Eng.* **2019**, *55*, 152−160.
(37) Burroughs, A. M.; Allen, K. N.; Dunaway-Mariano, D.; Aravind, L. Evolutionary Genomics of the HAD Superfamily: Understanding the Structural Adaptations and Catalytic Diversity in a Superfamily of Phosphoesterases and Allied Enzymes. *J. Mol. Biol.* **2006**, *361*, 1003−1034.
(38) Huang, H.; Pandya, C.; Liu, C.; Al-Obaidi, N. F.; Wang, M.; Zheng, L.; Toews Keating, S.; Aono, M.; Love, J. D.; Evans, B.; Seidel, R. D.; Hillerich, B. S.; Garforth, S. J.; Almo, S. C.; Mariano, P. S.; Dunaway-Mariano, D.; Allen, K. N.; Farelli, J. D. Panoramic View of a Superfamily of Phosphatases through Substrate Profiling. *Proc. Natl. Acad. Sci. U. S. A.* **2015**, *112*, 1974−1983.
(39) Zallot, R.; Oberg, N.; Gerlt, J. A. The EFI Web Resource for Genomic Enzymology Tools: Leveraging Protein, Genome, and Metagenome Databases to Discover Novel Enzymes and Metabolic Pathways. *Biochemistry* **2019**, *58*, 4169−4182.
(40) Zhang, Y.-H. P.; Myung, S.; You, C.; Zhu, Z.; Rollin, J. A. Toward Low-Cost Biomanufacturing through *in vitro* Synthetic Biology: Bottom-up Design. *J. Mater. Chem.* **2011**, *21*, 18877−18886.
(41) Zhang, Y.-H. P.; Lynd, L. R. Determination of the Number-Average Degree of Polymerization of Cellodextrins and Cellulose with Application to Enzymatic Hydrolysis. *Biomacromolecules* **2005**, *6*, 1510−1515.
(42) Van Overtveldt, S.; Verhaeghe, T.; Joosten, H. J.; van den Bergh, T.; Beerens, K.; Desmet, T. A Structural Classification of Carbohydrate Epimerases: From Mechanistic Insights to Practical Applications. *Biotechnol. Adv.* **2015**, *33*, 1814−1828.
(43) Jeon, B.-S.; Taguchi, H.; Sakai, H.; Ohshima, T.; Wakagi, T.; Matsuzawa, H. 4-α-Glucanotransferase from the Hyperthermophilic Archaeon *Thermococcus Litoralis*. *Eur. J. Biochem.* **1997**, *248*, 171−178.
(44) Zhou, W.; Huang, R.; Zhu, Z.; Zhang, Y.-H. P. J. Coevolution of Both Thermostability and Activity of Polyphosphate Glucokinase from *Thermobifida Fusca* YX. *Appl. Environ. Microbiol.* **2018**, *84*, e01224−e01218.
(45) Hsu, C.-C.; Hong, Z.; Wada, M.; Franke, D.; Wong, C.-H. Directed Evolution of D-Sialic Acid Aldolase to L-3-Deoxy-Manno-2-Octulosonic Acid (L-KDO) Aldolase. *Proc. Natl. Acad. Sci. U. S. A.* **2005**, *102*, 9122.
(46) Chen, C.-Y.; Georgiev, I.; Anderson, A. C.; Donald, B. R. Computational Structure-Based Redesign of Enzyme Activity. *Proc. Natl. Acad. Sci. U. S. A.* **2009**, *106*, 3764.
(47) An, H.; Song, J.; Wang, T.; Xiao, N.; Zhang, Z.; Cheng, P.; Ma, S.; Huang, H.; Chen, Y. Metal-Organic Framework Disintegrants: Enzyme Preparation Platforms with Boosted Activity. *Angew. Chem., Int. Ed.* **2020**, *59*, 16764−16769.
(48) Li, Q.; Fan, F.; Wang, Y.; Feng, W.; Ji, P. Enzyme Immobilization on Carboxyl-Functionalized Graphene Oxide for Catalysis in Organic Solvent. *Ind. Eng. Chem. Res.* **2013**, *52*, 6343−6348.
(49) Akgöl, S.; Öztürk, N.; Denizli, A. New Generation Polymeric Nanospheres for Catalase Immobilization. *J. Appl. Polym. Sci.* **2009**, *114*, 962−970.
(50) Jia, J.; Zhang, W.; Yang, Z.; Yang, X.; Wang, N.; Yu, X. Novel Magnetic Cross-Linked Cellulase Aggregates with a Potential Application in Lignocellulosic Biomass Bioconversion. *Molecules* **2017**, *22*, 269−282.
(51) Sun, S.; Wei, X.; Zhou, X.; You, C. Construction of an Artificial *in vitro* Synthetic Enzymatic Platform for Upgrading Low-Cost Starch to Value-Added Disaccharides. *J. Agric. Food Chem.* **2021**, *69*, 302−314.

https://doi.org/10.1021/acscatal.0c05718
ACS Catal. 2021, 11, 5088−5099